Surface alloy formation of Fe on Cr(100) studied by scanning tunneling microscopy

Y. J. Choi, I. C. Jeong,* J.-Y. Park, S.-J. Kahng, J. Lee, and Y. Kuk†
National Creative Research Initiatives, Center for Science in Nanometer Scale and Department of Physics, Seoul National University, Seoul 151-742, Korea

(Received 2 March 1998; revised manuscript received 28 October 1998)

Surface alloy formation of Fe on a Cr(100) surface was studied using a UHV scanning tunneling microscope. As we deposited Fe of less than 1 ML at room temperature and subsequently annealed the substrate at temperatures between 200 °C and 300 °C, we observed that Fe atoms incorporate into the Cr(100) surface, forming a well-ordered surface alloy of $Fe_{0.5}Cr_{0.5}$. These two elements were differentiated by imaging at the bias voltages near their surface states. The surface alloying was also confirmed by imaging at the bias voltages of their Shockley image states. By annealing the Fe layer of ~1 ML at 250 °C, we found that the solubility of Fe into the Cr(100) surface is ~25% at that temperature. Fe overlayer shows kinetically roughened mound structure at room temperature while it shows equilibrium two-dimensional islands at 300 °C.
[S0163-1829(99)06115-9]

INTRODUCTION

In the last decade, there has been great interest in the study of thin metal films to understand their versatile chemical, electronic, and magnetic properties. It has been known that the structure of a film interface plays an important role in defining its property. Many metallic films are known to grow in three different modes, depending on lattice mismatch and lattice structure: the Frank van der Merwe mode (layer-by-layer growth), the Volmer-Weber mode [three dimensional (3D) island growth], and the Stranski Krastanov mode (layer growth, followed by 3D growth). These three modes are classified under the assumption of negligible solubility between the overlayer and the substrate.[1] But, in many other cases of metallic films, their interface structures are not abrupt because of the intermixing between the overlayers and the substrates, although they are immiscible or their solubilities are quite low in their binary bulk-phase diagrams.[2–9] Recently, scanning tunneling microscope (STM) and total-energy calculation have revealed that metal-on-metal growth modes are much more complex than three growth modes.[2,4,6,7,10] Especially using STM, the initial stages of alloy formation at the atomic level could be observed directly in a number of metal-on-metal systems.[2–8,11–15]

STM, with scanning tunneling spectroscopy, can be utilized to identify alloy species during the formation process, as well as to image the surface geometrical structure. In the cases where the lattice mismatch between two materials is somewhat large or their valence band structures are different, each species in the alloyed phase could be identified with apparent difference in the STM images.[2–7,11–15] However, in cases where the lattice mismatch between two materials is not large, it is difficult to identify two species from the simple STM images. Recently, Davies *et al.* reported that different chemical species could be identified with the localized surface states of the two elements in the Cr on Fe(001) system, where the lattice mismatch is less than 0.6%.[8] The Cr on Fe(100) system has been widely investigated for its unusual magnetic properties and its application for a giant magnetoresistance (GMR) sensor as a form of a Fe/Cr/Fe multilayer.[16] Some magnetic anomalies, such as a surprisingly high magnetic moment of Cr at ~0.1 ML,[17] the unexpected phase of the antiferromagnetic ordering in the Cr layer, and the delayed onset of the antiferromagnetic ordering in the Fe/Cr/Fe sandwich structure,[18] were explained with interface alloying between the Cr overlayer and the Fe substrate at the growth temperature.[19] Although Cr can dissolve into the Fe matrix only up to 3% at 300 °C in the bulk-phase diagram,[20] it was reported that the solubility of Cr in Fe at the interface is higher than that in the bulk.[19] There have been many studies on the Cr film on a single crystal Fe(100) substrate, but there have been few studies on the opposite case, Fe film on a single-crystal Cr(100) substrate, because of the difficulty in cleaning a Cr substrate.[21] Although the bulk-phase diagram shows very similar solubility in Fe rich and Cr rich dilute alloys at 300 °C, the surface alloying was predicted and confirmed only when Cr is grown on Fe substrate. Despite this prediction, there are some cases where the surface alloying occurs in both dilute alloys.[22]

In this paper, we show that the surface-alloy formation can also occur at the low Fe coverage on the Cr(100) surface after Fe is deposited at room temperature and subsequently annealed the sample at temperatures between 200 °C and 300 °C. Incorporated Fe atoms are identified by the difference in tunneling currents at the bias voltage of the Cr surface state and at that of the Fe surface state. The alloyed area can also be differentiated by measuring the change of the work function at the alloyed region from that at a bare Cr surface. In addition to the alloy formation at the low Fe coverage, we observed that layer-by-layer growth of Fe layers can be achieved at the Fe coverage of ~1 ML by annealing the sample at 250 °C.

EXPERIMENT

A clean Cr surface was prepared by repeated cycles of Ar ion sputtering and annealing in an ultrahigh vacuum chamber with the base pressure of $<1.5\times10^{-10}$ Torr. It is well known that obtaining an adsorbate-free (especially nitrogen),

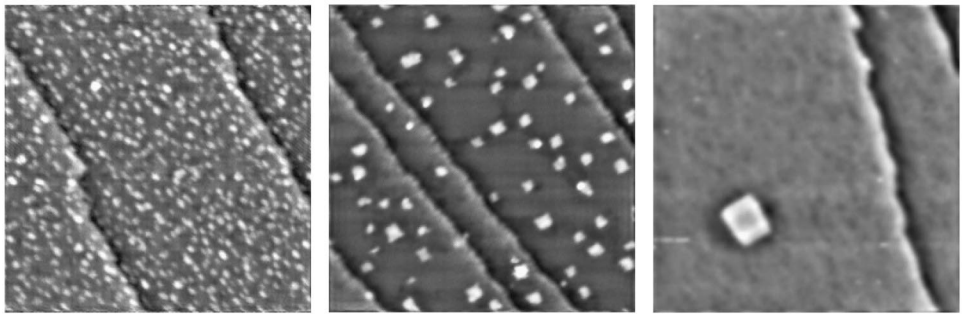

FIG. 1. Change of the morphology of the Fe overlayer as a function of subsequent annealing temperature in the low coverage of Fe. The density and total area of islands decrease as the islands grow to rectangular shape with increasing annealing temperature, T. (a) T = room temperature, (b) $T=200\,^{\circ}\mathrm{C}$, (c) $T=300\,^{\circ}\mathrm{C}$. All the images were taken at $V_s=-2$ V and the image sizes are 350×350 Å.

clean Cr surface is difficult.[21] Insufficient sputtering and annealing results in a nitrogen-induced superstructure. We were able to decrease impurity levels below 0.3% at the surface by sputtering and annealing up to 900 °C for several months, as monitored by low energy electron diffraction (LEED), Auger electron spectroscopy, and STM. After the clean surface was obtained, Fe was deposited at room temperature by directly heating a 99.99% Fe wire with the deposition rate of ~1 ML/min. In order to study alloying of Fe into the Cr substrate, the sample was annealed subsequently at the various temperatures for 10 min each time. The temperature of the sample was measured by an optical pyrometer and the uncertainty in the temperature measurements is $\pm10\,^{\circ}\mathrm{C}$. The STM images were obtained after cooling down the sample to the room temperature over a period of an hour. The detailed design of UHV STM used in this paper can be found elsewhere.[23] But briefly, the system is equipped with UHV STM, LEED, and Auger electron spectroscopy. STM images were obtained at various tunneling voltages in order to identify chemical species on the surface.

RESULTS AND DISCUSSION

When Fe was deposited on the Cr(100) surface at room temperature, heterogeneous nucleation of Fe was observed near defects. Figure 1 shows the change of the morphology as a function of subsequent annealing temperature at the low Fe coverage. The density and the total area of islands decreases and the islands grow to rectangular shapes as the annealing temperature is raised. There are two possibilities to explain this phenomenon; (1) Fe atoms reevaporate at the annealing temperature, or (2) Fe atoms incorporate into the Cr substrate. Since the Fe Auger signal was nearly unchanged during and after annealing, it was concluded that Fe incorporation into Cr is far more probable. Since Fe has a localized surface state just above the Fermi level and Cr has one just below the Fermi level, one can distinguish Fe atoms from the Cr substrate if the tunneling voltage is set at the Fe surface state. Since the images in Fig. 1 were taken at the sample bias voltage (V_s) of -2 V and those in Fig. 2 were taken at 0.3 V (close to the Fe surface state), more visible atomic rows in Fig. 2 are believed to be incorporated Fe atoms. Although they are clearly visible, their heights are much lower than those of 1 ML Fe islands, indicating that the rows are not from the physical protrusion but from their electronic property. The atomic rows start from island or step edges and there is no region where they are nucleated on the terrace. If steps or island edges may work as the reaction sites for incorporation of adatoms into the substrate, the alloying would start from those sites. Based on many observed STM images, there is a strong tendency that the ratio of the total amount of Fe atoms as pure Fe islands to incorporated Fe atoms decreases with decreasing terrace width. It confirms the fact that alloying starts from step edges because

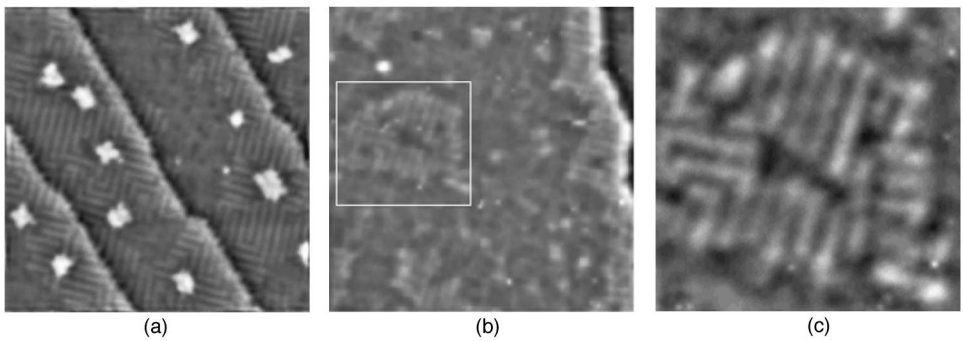

FIG. 2. Surface alloy by incorporation Fe atoms into Cr matrix. There can be seen the Fe atomic rows, which are brighter than Cr bare terraces and darker than Fe islands with 1-ML height. The incorporation of Fe atoms started from island or step edges. When the annealing temperature is 300 °C, the alloyed area was found on the terrace. (a) $T=200\,^{\circ}\mathrm{C}$, (b) $T=300\,^{\circ}\mathrm{C}$, (c) close-up view of the alloyed area in (b). All the images were taken at the Fe surface state ($V_s=0.3$ V) and the image sizes are 180×180 Å except (c). Additional black and white lines appear along the step edges in the process of enhancing the image contrast.

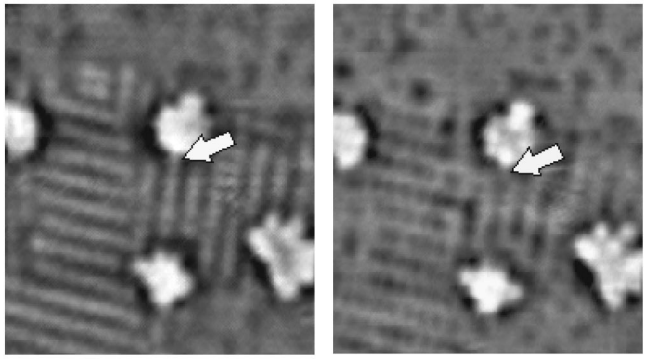

FIG. 3. Identification of different elements in the alloyed regions using surface states. (a) $V_s = 0.3$ V (Fe surface state), (b) $V_s = -0.2$ V (Cr surface state). The contrast of the atomic row marked by an arrow is reversed as the sample bias is changed from 0.3 to -0.2 V. The image sizes are 80×90 Å and $T = 200$ °C.

there are effectively more defect sites in narrow terraces for alloying at the step edges. As we raised the annealing temperature up to 300 °C, the alloyed region on the terrace can be found. The region is thought to be the region where Fe islands existed at lower temperature and the Fe island is now fully incorporated into the Cr substrate at 300 °C.

For incorporated Fe atomic rows, their contrast would be reversed as the sample bias is changed from the Fe surface state ($V_s = 0.3$ V) to the Cr surface state ($V_s = -0.2$ V). Figure 3 shows this phenomenon dramatically. Figures 3(a) and 3(b) show the STM images taken at sample bias voltages of the Fe and Cr surface states, respectively. The contrast of the atomic row marked by an arrow is reversed as the sample bias is changed from 0.3 to -0.2 V. From this observation, we can conclude that Fe atoms incorporate into the Cr substrate to form a well-ordered surface alloy at the annealing temperature of 200 °C.

When Cr atoms diffuse into the Fe matrix, they form a disordered isomorphic alloy.[8] However, the observed Fe atomic rows indicate an ordered alloy formation as we grow Fe on a Cr(100) substrate. The driving forces for the surface-alloy formation have been attributed to their lattice mismatch and difference in their surface-free energies. Since the lattice mismatch between Fe (2.87 Å) and Cr (2.88 Å) is small,[24] the difference in the surface-free energies between Fe and Cr may play a significant role in this case. Although simple thermodynamic arguments have been successful in explaining surface-alloy formation in many binary cases, recent STM studies and total energy calculations show that the naïve surface-free energy argument is inadequate for some cases.[2,6,7,10] From the coherent-potential approximation and effective-medium theory (EMT) calculation, Christensen *et al.* constructed surface-phase diagrams for all transition- and noble-metal combinations for close-packed surfaces of the equilibrium structure of the host metal as a function of the surface composition.[10] Their results successfully explain many STM results of alloys including the Cr/Fe(100) system, although the present face (100) is not a close-packed plane. In the view of their results, it was proposed that Fe cannot alloy with the Cr substrate. However, since their general calculation is restricted to the zero temperature limit, the temperature dependence of the phase diagram should be considered with care in each case. It should be also noted that surface-alloy formation is promoted only above 200 °C in the Cr/Fe(100) case from the former results.[25] Therefore, it may be inferred that Fe atoms with enough thermal energy will incorporate into the Cr matrix near the island edges and Cr atoms substituted by Fe atoms diffuse towards the edges of the upper terrace to form the surface alloy near the step edges. From the STM images at two surface states, we propose a structural model of the surface $Fe_{0.5}Cr_{0.5}$ alloy in which Fe and Cr rows alternate.

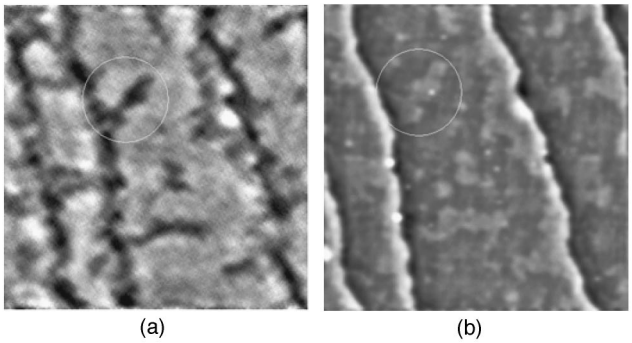

FIG. 4. The depressed tunneling probability of the alloyed regions when the image is taken above the vacuum level of Cr at (a) $V_s = 5.5$ V, compared to the Fe surface state at (b) $V_s = 0.3$ V. The image sizes are 350×350 Å and $T = 300$ °C.

It was reported that elemental contrast in an STM can be obtained from the different local work function of the different elements.[26] As the bias voltage of STM is set near the vacuum level, a Rydberg-type series of resonance states may enhance the tunneling probability. They can be regarded as image states modified by the field of the tip. While the lowest level of the image states is known to be bound by 0.85 eV below vacuum level from a simple model,[27] the field applied by the tip shifts the lowest level of the image states slightly above the work function. Since the image states are tied to the local work function of a material, it is possible to obtain elemental contrast in STM by switching the tip bias between image states of different materials. Recently, the chemical identification of Cu stripes formed along the surface steps of vicinal Mo(110) was achieved by using the different image states resulting from the different work functions.[26] Since Fe and Cr are very similar in their work functions, it is expected that their chemical identification may not be possible. At the same time, atomically resolved STM images are hardly obtained when the tunneling bias is set near the vacuum level due to the large tunneling gap. However, the work function of an ordered alloy is known to be varied as a function of the compositional ratio between two elements and may have a local minimum at a specific composition.[28] Therefore, the work function of the well-ordered alloy in Fe/Cr(100) can be considerably different from that of Fe or Cr. Figure 4(a) shows the depressed tunneling probability of the alloyed region when the image was taken just above the Cr vacuum level. While the alloyed regions look brighter than the bare Cr surface in Fig. 4(b), which was taken at the Fe surface state, the contrast is reversed when the image was taken above the Cr vacuum level. From these observations, it is proven that Fe makes an alloy with the Cr substrate and the

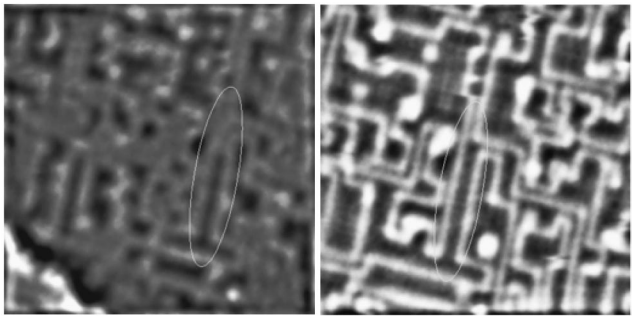

FIG. 5. The nitrogen-induced structure of Cr(100) surface, at (a) $V_s = -0.2$ V, (b) $V_s = 0.3$ V. The image sizes are 110×110 Å.

local barrier height of the alloy is quite different from that of the substrate.

The structure of the alloy resembles that of the nitrogen-induced Cr(100) surface, which was recently reported by Schmid *et al.*[29] They observed that nitrogen induces the reconstruction of the Cr(100) surface and the reconstructed structure changes as a function of the concentration of segregated nitrogen on the Cr surface. The proposed structure changes from the clean Cr (1×1) to the *N*-rich (1×1) via $c(2\times2)$ and $c(3\sqrt{2}\times\sqrt{2})$ $R\pm45°$ with increasing coverage of *N*. When the *N* coverage is above 0.5 ML, line-shaped domain boundaries are observed. Similar results were also observed in the process of cleaning the Cr surface. When the nitrogen is not fully depleted from the Cr surface, which can be monitored from Auger electron spectroscopy, there appear atomic rows similar to the Fe atomic rows in the surface alloy of the Fe/Cr(100) system. In spite of the similarity in their shapes, there still remain a couple of remarkable differences. One is the ordering of the spacing of atomic rows and the other is the dependence of its contrast on the bias voltages. While the rows in the surface alloy are well ordered, those in the *N*-induced structure are arbitrarily arranged with a great deal of disorder. Although there are also atomic rows similar to those in the Fe/Cr alloy, their spacings are not uniform compared to the case of the Fe/Cr alloy. The bias voltage dependence of the contrast of the rows is quite different from that in the Fe/Cr alloy. The contrast of the atomic rows is enhanced when the image is taken at the Cr surface state, and there is no contrast inversion when the bias voltage is changed from the Fe surface state to the Cr surface state, as shown in Fig. 5.

When ~1 ML Fe is deposited at room temperature, the Fe island grows into the mound shape of similar size, which resembles the feature during the Fe(001) homoepitaxy.[30] The origin of the mound shape of islands was explained by the difference of energy barrier between the transport of diffusing atoms downward over the island edge and the usual surface diffusion on the island. If the thermal energy is large enough to overcome the energy barrier for the descending of the diffusing atoms over the island edge, a two-dimensional island will be formed. In this paper, the kinetic energy of Fe atoms can be increased by the postannealing. As the sample is postannealed at 250 °C for 10 min, the coalescence of Fe islands is observed in addition to the flattened shape of Fe islands. While the coverage calibrated from the deposition rate is 0.8 ML, the coverage estimated from the STM images when the coalescence occurs is about 0.55 ML, suggesting that the solubility of Fe into the Cr(100) surface at 250 °C is about 25%. The enhancement of the solubility in the surface alloying compared to the bulk case is consistent with the Cr on Fe(100) case.[19] When the annealing temperature is raised up to 300 °C, the diffusivity of Fe atoms on the Cr surface is large enough and the boundary of the Fe layer goes along highly symmetric ⟨100⟩ directions. The seemingly negative islands on the terrace in Fig. 6(c) are the exposed areas of the Cr substrate, which is surrounded by the Fe overlayer. Unexpectedly, there is no indication of well-ordered alloy formation in that area, as well as there is no evidence of alloy formation on the Fe overlayer. From these facts, it can be inferred that incorporation of Fe into the Cr surface at the high-coverage regime mainly occurs at the interface between the Fe overlayer and the Cr substrate.

CONCLUSION

While Cr alloys with an Fe substrate without any ordering at the interface of Cr/Fe(100),[8] we found that Fe atoms incorporate into the Cr surface and form a well-ordered alloy at the elevated sample temperature at the low-coverage regime of Fe. The compositional ratio between Fe and Cr in the surface alloy is 1:1. We distinguished the Fe atomic rows from the Cr rows in the Fe/Cr surface alloy, by imaging at the bias voltages of the surface states of two elements. In

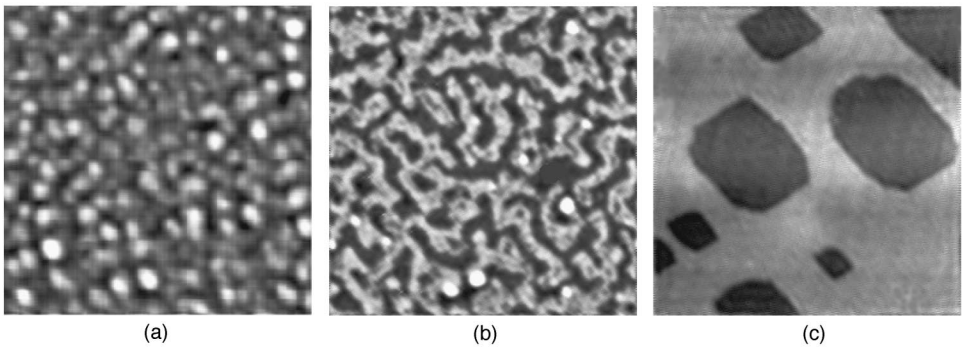

FIG. 6. Change of the morphology of the Fe overlayer from the kinetically roughened mound structure to the equilibrium two-dimensional island by raising annealing temperature. (a) T = room temperature, (b) $T = 250$ °C, (c) $T = 300$ °C. All the images were taken at $V_s = -2$ V. The image sizes are 180×180 Å for (a) and 350×350 Å for (b) and (c).

addition, the work function at the alloyed regions is somewhat different from that at a bare Cr surface, which can be inferred from the lower tunneling probabilities observed at the Cr image states.

When we deposit Fe around 1 ML and anneal the sample up to 300 °C, Fe atoms are dissolved into the Cr surface about 25% and the boundaries of the Fe overlayer go along the crystalline symmetric axis ⟨100⟩. Contrary to the low-coverage regime, there is no indication of well-ordered alloy formation in the exposed Cr surface. While an alloyed appearance is observed at the Cr coverage of 2–3 ML in the Cr on Fe(100) case,[19] the alloying is observed to be confined only to the interface of Fe/Cr(100).

ACKNOWLEDGMENTS

This paper was partially supported by the Ministry of Education, Korea through Grant No. BSRI-97-2416, the Korean Science and Engineering Foundation through Grant No. 961-0207-072-2, and the national creative research initiative in Korea.

*Present address: Hyundai Electronics Industries Co. LTD, Ichon, Kyoungki-do, 467-701, Korea.

†Author to whom correspondence should be addressed. Electronic address: ykuk@phya.snu.ac.kr

[1] E. Bauer and Jan H. van der Merwe, Phys. Rev. B **33**, 3657 (1986).

[2] I. Pleth Nielsen, F. Besenbacher, I. Stensgaard, E. Lægsgaard, C. Engdahl, P. Stoltze, K. W. Jacobsen, and J. K. Nørskov, Phys. Rev. Lett. **71**, 754 (1993).

[3] C. Nagl, O. Haller, E. Plazgummer, M. Schmid, and P. Varga, Surf. Sci. **321**, 237 (1994).

[4] C. Nagl, E. Plazgummer, M. Schmid, P. Varga, S. Speller, and W. Heiland, Phys. Rev. Lett. **75**, 2976 (1995).

[5] Markus B. Hugenschmidt, Andreas Hitzke, and R. Jürgen Behm, Phys. Rev. Lett. **76**, 2535 (1996).

[6] P. T. Sprunger, E. Lægsgaard, and F. Besenbacher, Phys. Rev. B **54**, 8163 (1996).

[7] H. Röder, R. Schuster, H. Brune, and K. Kern, Phys. Rev. Lett. **71**, 2086 (1993).

[8] A. Davies, J. A. Stroscio, D. T. Pierce, and R. J. Celotta, Phys. Rev. Lett. **76**, 4175 (1996).

[9] J. Tersoff, Phys. Rev. Lett. **74**, 434 (1995).

[10] A. Christensen, A. V. Ruban, P. Stoltze, K. W. Jacobsen, H. L. Skriver, J. K. Nørskov, and F. Besenbacher, Phys. Rev. B **56**, 5822 (1997).

[11] D. D. Chambliss and S. Chiang, Surf. Sci. Lett. **264**, L187 (1992).

[12] C. Nagl, E. Plazgummer, O. Haller, M. Schmid, and P. Varga, Surf. Sci. **331–333**, 831 (1995).

[13] R. G. R. van der Kraan and H. van Kempen, Surf. Sci. **338**, 19 (1995).

[14] P. W. Murray, S. Thorshaug, I. Stensgaard, F. Besenbacher, E. Lægsgaard, A. V. Ruban, K. W. Jacobsen, G. Kopidakis, and H. L. Skriver, Phys. Rev. B **55**, 1380 (1997).

[15] T. Flores, S. Junghans, and M. Wuttig, Surf. Sci. **371**, 14 (1997).

[16] L. M. Falicov, Phys. Today **45(x)**, 46 (1992).

[17] C. Turtur and G. Bayreuther, Phys. Rev. Lett. **72**, 1557 (1994).

[18] J. Unguris, R. J. Celotta, and D. T. Pierce, Phys. Rev. Lett. **67**, 140 (1991).

[19] A. Davies, J. A. Stroscio, D. T. Pierce, J. Unguris, and R. J. Celotta, J. Magn. Magn. Mater. **165**, 82 (1997).

[20] O. Kubaschewski, *Iron-Binary Phase Diagrams* (Springer-Verlag, Berlin, 1982).

[21] J. S. Foord and R. M. Lambert, Surf. Sci. **115**, 141 (1982).

[22] For example, Refs. 2 and 5 are the Au-Ni case, and Refs. 3 and 4 are the Pb-Cu case

[23] Y. Kuk and P. J. Silverman, Rev. Sci. Instrum. **60**, 165 (1989).

[24] C. Kittel, *Introduction to Solid State Physics*, 6th ed. (Wiley, New York, 1991), p. 23.

[25] D. T. Pierce, J. A. Stroscio, J. Unguris, and R. J. Celotta, Phys. Rev. B **49**, 14 564 (1994).

[26] T. Jung, Y. W. Mo, and F. J. Himpsel, Phys. Rev. Lett. **74**, 1641 (1995).

[27] N. V. Smith, Phys. Rev. B **32**, 3549 (1985).

[28] A. Kiejna and K. F. Wojciechowski, *Metal Surface Electron Physics* (Alden, Oxford, 1996), p. 94.

[29] M. Schmid, M. Pinczolits, W. Hebenstreit, and P. Varga, Surf. Sci. **377-379**, 1023 (1997).

[30] J. A. Stroscio, D. T. Pierce, M. D. Stiles, A. Zangwill, and L. M. Sander, Phys. Rev. Lett. **75**, 4246 (1995).